Cell swelling enhances GPCR ternary complex formation, underpinning the potentiation of β2 adrenergic receptor-mediated cAMP response

Alexei Sirbu[1], Marc Bathe-Peters [1], Asuka Inoue[2], Martin J. Lohse[3,4], Paolo Annibale[1,5]*

[1] Max Delbrück Center for Molecular Medicine in the Helmholtz Association (MDC), 13125 Berlin, Germany

[2] Tohoku University, 980-8578 Japan

[3] ISAR Bioscience Institute, 82152 Munich-Planegg, Germany

[4] Leipzig University, Medical Faculty, Rudolf-Boehm-Institute of Pharmacology and Toxicology, 04107 Leipzig, Germany

[5] School of Physics and Astronomy, University of St Andrews, KY169SS St Andrews, United Kingdom

*paolo.annibale@mdc-berlin.de

Abstract

G protein-coupled receptors conformational landscape can be affected by their local, microscopic interactions within the cell plasma membrane. We employ here a pleiotropic stimulus, namely osmotic swelling, to alter the cortical environment within intact cells and monitor the response in terms of receptor function and downstream signaling. We observe that in osmotically swollen cells the β2-adrenergic receptor, a prototypical GPCR, favors an active conformation, resulting in cAMP transient responses to adrenergic stimulation that have increased amplitude. The results are validated in primary cell types such as adult cardiomyocytes, a model system where swelling occurs upon ischemia-reperfusion injury. Our results suggest that receptor's function is finely modulated by their biophysical context, and specifically that osmotic swelling acts as a potentiator of downstream signaling, not only for the β2-adrenergic receptor, but also for other receptors, hinting at a more general regulatory mechanism.

Introduction

One of the tenets in G protein-coupled receptors (GPCR) pharmacology is the ternary complex model, stating that a high affinity state characterized by increased receptor-G protein coupling also correlates to increased affinity of the receptor towards its agonist, since the intracellular G protein coupling stabilizes the active receptor conformation[1]. Further to the development of this model, our understanding of GPCRs function has evolved from two-state switches to rheostats exploring a complex conformational landscape, that in turn entails a broad repertoire of intracellular interactions[2]. Prototypical examples are molecules from the extracellular space acting as allosteric modulators of receptor function: they favor specific conformations -further stabilized upon ligand binding- that are different from those that would be observed in the absence of the modulator[3]. An emerging concept is that changes of the biophysical context around the receptor can 'allosterically' modulate its function. Mechanistically this involves the action of accessory proteins[4], local lipid composition[5], interaction with intracellular scaffolds[6], and -as highlighted recently- local curvature[7]. These interactions can modulate each of the canonical signaling steps (ligand binding, ternary complex formation with cognate G protein, β-arrestin recruitment, trafficking), endowing these receptors with a broad modulatory repertoire able to nuance specific signals in a dynamic and flexible way in space and time.

Some of these interactions may be receptor-specific and associated with specific modulatory proteins, such as Receptor Associated Modifying Proteins (RAMPs)[4]. Other interactions may

be more diffuse, such as the interaction of GPCRs containing a PDZ binding sequence with the cortical actin, or, as it was proposed more recently, the segregation of selected GPCRs to areas of higher or shallower curvature within the cell membrane[8]. Along these lines, we observed recently µm-sized receptor-specific segregation to a subcellular compartment, such as the T-tubular network of adult cardiomyocytes, characterized by high local curvature[9].

While the hypothesis that subcellular receptors localization may indeed modulate -to a sizable extent- their behavior[10] is being increasingly tested, nonetheless the molecular mechanisms underpinning such effects are harder to unravel. These may be ascribed to heterogeneities in lipid composition of the plasma membrane[11], in the local density of the cortical actin network and the variability of its interactions with the membrane[12]. Moreover, if modulation of GPCR signaling indeed occurs across multiple length-scales at the plasma membrane, from nanometer to micrometer scale, its microscopic identification challenges current technologies[13].

We reasoned that osmotic swelling, a process that occurs in several physiological settings may offer the type of pleiotropic biophysical modulation that we are seeking to test this hypothesis. Cell swelling is associated to a complex rearrangement of the cell membrane environment, ranging from alteration of local geometry, F-actin remodulation and, increases in cell surface originating from flattening of the membrane, not unlike ironing out wrinkles in a cloth.

We decided to focus on β-Adrenergic Receptors (β-ARs), both because of their prototypical nature (i.e. they couple to the stimulatory G protein and elicit an increase in cAMP upon $G\alpha_s$ interaction with the adenylate cyclase (AC)) but also because they display a rich conformational landscape[14] and the role of cortical actin in connection to their localization and signaling, in particular the β2-AR, is well documented[6,15].

Our key observation is that swollen cells yield sizably higher cAMP concentrations in response to β-ARs stimulation than non-swollen cells. To pinpoint at what step this occurs, we set to explore the whole signaling cascade of the β2-AR. Each step of the signaling cascade was investigated with a specific fluorescent spectroscopy method, ranging from TIRF to fluorescence polarization and FRET biosensing, that allowed us working in intact cells. We could determine that this effect does not arise from alterations at the level of AC catalytic rates, nor by alterations of receptors trafficking, but rather by a distinctive increase in receptor-G protein coupling, mirrored by an increased affinity of the agonist isoproterenol for the receptor.

These findings demonstrate a novel way of modulating GPCR conformation by biophysical factors, while also showing a previously unappreciated effect of cell swelling on 2nd messenger production, which has the potential to be transferred to other GPCRs or transmembrane receptors acting in a broad range of physiological settings.

Results

To size the effect of osmotic swelling on the downstream signalling cascade of the β-ARs we first employed FRET-based cAMP fluorescence biosensors. The layout of our readout is schematically depicted in **Figure 1a**. When measuring FRET in a single cell under a microscope, it is possible to display the degree of FRET between the donor and acceptor of the sensor in a false color scale, that will change upon agonist addition (100 pM Isoproterenol (Iso) in our case). The relative change between the swollen and control state of representative HEK293 cell is displayed in **Figure 1b**, next to the donor and acceptor channels separately. Upon addition of the swelling medium (containing the same concentration of Iso as the isotonic medium) to a cell expressing endogenous levels of receptors, the cAMP response is sizably increased. We then moved to a high-throughput configuration where the signal from tens of

thousands of cells was observed in 96-well plates using a fluorescent plate reader. A representative trajectory of intracellular cAMP concentration (proportional to the change in normalized FRET ratio) upon Iso addition in control vs swollen cells is displayed in **Figure 1c**. Trajectories from swollen cells are displayed in blue throughout the manuscript, as opposed to cells maintained in isotonic medium (control) which are displayed in red. A strong peak in cAMP concentration is observed in the swollen cells a few minutes upon non-saturating Iso addition, which then declines to a steady state comparable to the concentration observed in the controls (**Supplementary Figure 1a**). Saturating cAMP levels are then obtained upon Fsk/IBMX stimulation for normalization purposes. When repeated for increasing concentrations of the agonist, ranging from 1 pM up to 100 nM concentration, it was thus possible to build a concentration response curve, as displayed in **Figure 1d**. We observe a statistically significant difference in the log(EC_{50}), which drops from -9.3 ± 0.1 to -9.84 ± 0.09 for the average curves. To rule out any effect of osmotic swelling on the readout of our fluorescence biosensor, a concentration response curve was calculated in the two conditions using the cell permeable cAMP derivative 8-Br-cAMP, displaying overlapping curves for swollen and control cells (**Supplementary Figure 1b**). Individual log(EC_{50}) values from separate experiments are displayed for the two conditions in **Figure 1e**, which in turn allows to appreciate the fact that the observed difference applies only to the transient cAMP response and not to the steady state concentration. Interestingly, similar results can be obtained when looking at cells stimulated with other β-adrenergic agonists, such as salbutamol, salmeterol and terbutaline (**Supplementary Figure 1 c-e**). When challenging other G_s coupled receptors endogenously found in HEK293 cells, such as the Histamine H_2 receptor or the melanocortin receptors **(Supplementary Figure 1 f-g)** a similar outcome in terms of cAMP response can be observed upon osmotic swelling. Moreover, we observe a similar behavior at the level of Gi protein activation[16] for the μ Opioid Receptor (μOR), upon stimulation with the synthetic agonist DAMGO (**Supplementary Figure 1 i-j)**.

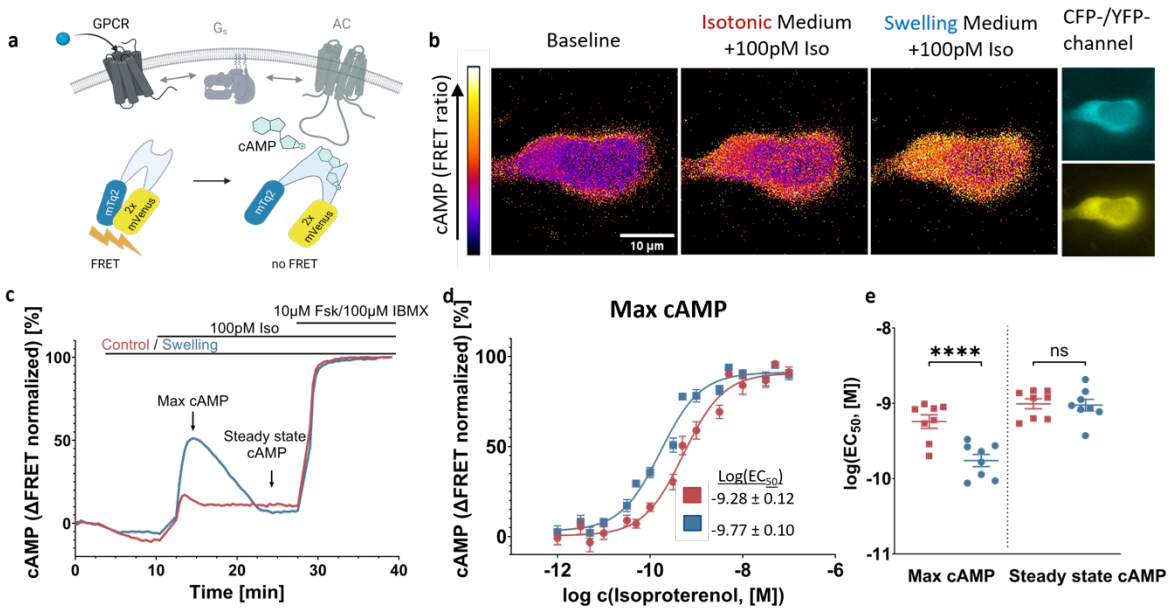

Figure 1 Cell swelling increases β-adrenergic-mediated cAMP production in HEK293 cells.

a Schematics of GPCR-mediated cAMP production and its detection by a FRET biosensor; **b** Representative images of a HEK293 cell stably expressing cytosolic Epac-S^{H187} [17] showing acceptor/donor ratio in false colour; the cells are exposed to 100 pM isoproterenol first in isotonic (300 mOsm) and subsequently in swelling medium (200 mOsm); **c** representative curve showing kinetics of acceptor/donor ratio measured in HEK293T cells stably expressing

Epac-S^{H187} in a microplate reader (normalized to baseline and 10μM Forskolin + 100μM IBMX); **d** averaged concentration response curves representing maximal cAMP concentrations, as indicated in (**c**) (mean ± SEM; n = 8 plates form 7 independent experiments); **e** $\log EC_{50}$ values from individual experiments comparing swelling and control condition for maximal and steady state cAMP concentrations (statistical analysis performed by a paired two-tailed t-test).

We then addressed the question if this remarkable behavior was observed also in primary cells, that are known to be subject to osmotic swelling in physiological or pathophysiological conditions, namely adult ventricular cardiomyocytes (CM). CMs undergo swelling during the reperfusion phase following ischemic shock[18]. Murine adult ventricular CMs were isolated and seeded on multiwell imaging plates and imaged on the same day, after labeling using a cell membrane dye (**Materials and Methods)**. Upon exposure to the swelling media the CMs display a visible increase in volume, as illustrated in **Figure 2a**. The increase was quantified as the relative change in cell area, as detected in 2D confocal sections (**Figure 2b, Supplementary Figure 2 a-d).** Following the same approach used to generate the data in **Figure 1b**, we employed CMs isolated from a transgenic mouse expressing the Epac1-camps cAMP sensor[19,20] and imaged them under a microscope (**Supplementary Movie 1**). The relative changes in cAMP concentration upon agonist addition were quantified for each cell, and representative traces for a control vs a swollen CMs are displayed in **Figure 2c**. Upon osmotic swelling, the cAMP response to non-saturating concentrations of Iso is clearly enhanced, consistent with the observations reported in **Figure 1** for HEK293 cells.

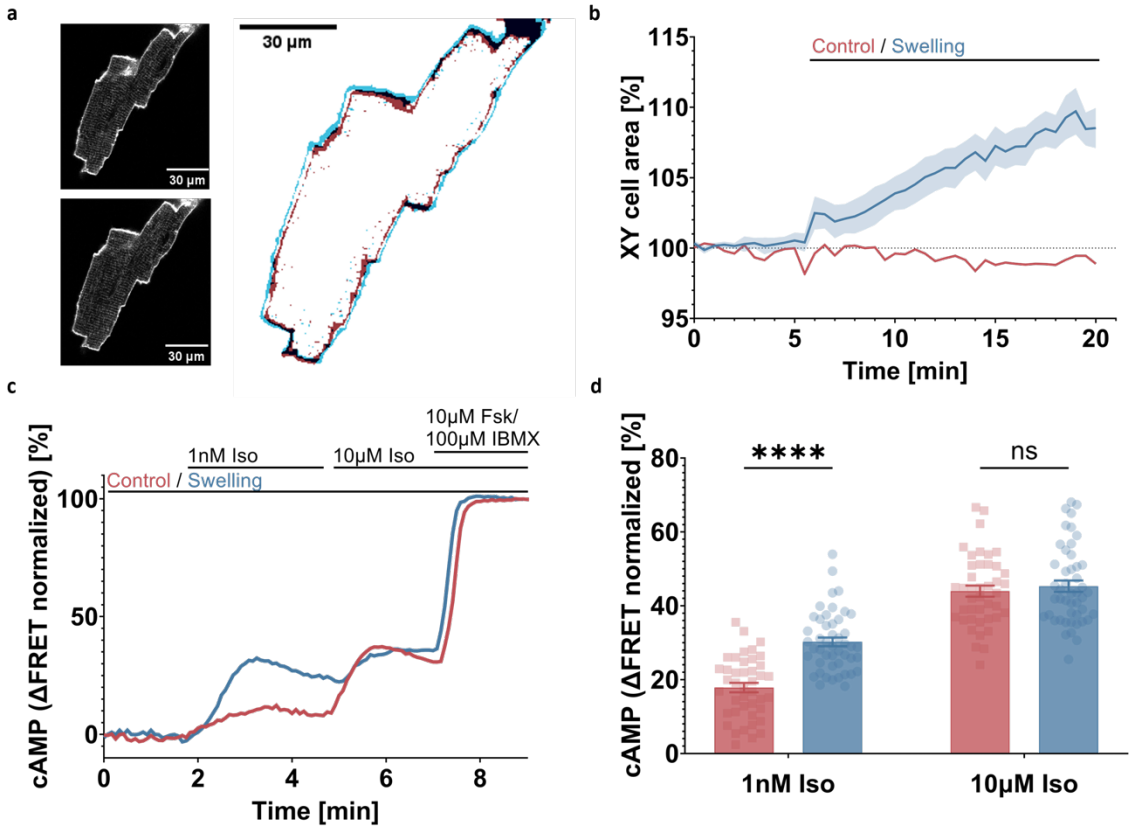

Figure 2 Cell swelling increases β-adrenergic mediated cAMP production in adult mouse ventricular cardiomyocytes (CM)

a Confocal images of CM under isotonic conditions (upper inset) and after 20 minutes of exposure to swelling medium (lower inset), with an overlay of cell edges under both conditions (main); **b** average curve showing the area of a confocal CM slice (mean ± SEM; n = 7 cells

from 3 independent experiments); **c** representative curve showing kinetics of acceptor/donor ratio measured in CM stably expressing Epac1-camps under an epifluorescence microscope (normalized to baseline and 10 μM Forskolin + 100 μM IBMX); **d** maximal cAMP concentrations reached upon stimulation with 1 nM and 10 μM isoproterenol respectively, normalized to 10 μM Forskolin + 100 μM IBMX (mean ± SEM; n = 42 (control) and 47 (swelling) cells from 3 independent experiments; statistical analysis performed by an unpaired two-tailed t-test).

The data for 10 nM and 10 μM iso additions are summarised in **Figure 2d**, and illustrate that cAMP signalling is enhanced in swollen adult CMs for Iso stimulations around the reported EC_{50}[17], while being equal at saturating concentration. Albeit it was not possible to generate a full concentration response curve based on single cell images, this data reports an effect clearly consistent with the one displayed in **Figure 1d**. Overall, these results point to the potential physiological relevance of this mechanism.

We thus set out to identify the molecular determinants of the observed changes in cAMP response in swollen cells. Since swelling is a pleiotropic modulator of cell homeostasis, we systematically investigated all steps of the signalling cascade, from PDE-mediated degradation of cAMP up to G protein coupling. We graphically summarised these steps in **Figure 3a**, that acts as a legend to the other panels of **Figure 3**. We first set to rule out that altered receptor trafficking, namely enhanced desensitization or downregulation supported by clathrin-mediated endocytosis could be the origin of the observed effect[21]. We treated cells with Dyngo-4a, a well characterised dynamin inhibitor. **Figure 3b** illustrates that the transient cAMP production increase reported in **Figure 1c** is still present in HEK293 cells treated with 10 μM Dyngo4a (the full concentration response curve is displayed in **Supplementary Figure 3a**). We then investigated the potential role of altered phosphodiesterase activity[22], as altered degradation rates (in this case reduced) may account for the observed increase in cAMP concentration transients in swollen cells.

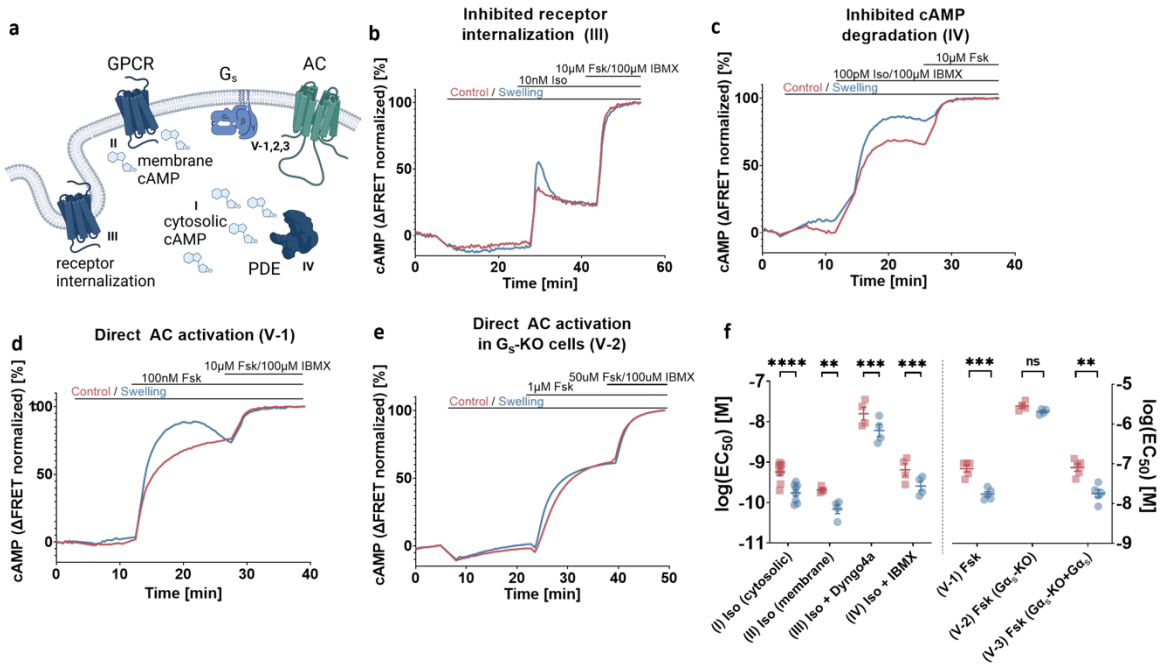

Figure 3 Impact of cell swelling on the molecular steps of the β-adrenergic signalling cascade

a Schematics of key steps of the signalling cascade that may be affected by swelling and were assessed under following conditions: (I) cytosolic cAMP upon Iso stimulation, (II) local cAMP at the plasma membrane upon Iso stimulation measured with an Epac-Camps1-Caax sensor, (III) cytosolic cAMP measured upon Iso stimulation after treatment with 10μM Dyngo4a for 30 min, (IV) cytosolic cAMP measured upon Iso stimulation with simultaneous addition of 100μM IBMX, (V-1,2,3) cytosolic cAMP measured upon Fsk stimulation in wt $G\alpha_s$ phenotype (V-1), $G\alpha_s$-KO cells (V-2) and $G\alpha_s$-KO cells transiently transfected with $G\alpha_s$ (V-3); **b** representative curve of FRET ratio reporting on the intracellular cAMP concentration under inhibition of receptor internalization using 10 μM Dyngo4a; **c** representative curve of intracellular cAMP concentration under inhibition of PDE activity by 100 μM IBMX; **d** representative curve of FRET ratio reporting intracellular cAMP concentration upon direct stimulation of ACs by 100nM Forskolin; **e** representative curve of FRET ratio reporting on intracellular cAMP concentration upon direct stimulation of ACs by 1μM Forskolin in a $G\alpha_s$ knockout cell line transiently transfected with Epac1-S^{H187}; **f** $\log EC_{50}$ values from individual experiments comparing swelling and control condition for maximal cAMP concentrations under conditions listed in **(a)** (statistical analysis performed by a paired two-tailed t-test).

The addition of the pan-PDE inhibitor IBMX, at the saturating concentration of 100 μM, did not abolish the observed relative increase in transient cAMP concentration in the swollen cells, as illustrated in **Figure 3c** and **Supplementary Figure 3b**. Similarly, the localization of the sensor did not seem to affect the outcome, since a membrane bound cAMP sensor[23] also confirmed the observed effect (**Supplementary Figure 3c**). We thus moved upstream along the signalling cascade: the next target is the family of enzymes responsible for cAMP synthesis, namely ACs. ACs are canonically activated by the GTP-bound $G\alpha_s$ subunit of the heterotrimeric G protein. However, the diterpene Forskolin and $G\alpha_s$ have a synergistic/cooperative action in activating ACs. In cells possessing endogenous $G\alpha_s$, direct stimulation of AC by Forskolin leads to marked cAMP concentration increases, and the differential effect elicited by cell osmotic swelling persists (**Figure 3d and Supplementary Figure 3d**). However, interestingly, in cell lines carrying a $G\alpha_s$ knockout[24], we observed that any effect of osmotic swelling upon the amplitude or kinetics of the cAMP concentration increase (**Figure 3e and Supplementary Figure 3e**) is lost. The effect is however recovered upon heterologous transfection of $G\alpha_s$ in the knockout lines (**Figure 3f and Supplementary Figure 3f**), thus pinning on the alpha subunit of the heterotrimeric G protein a key role in modulating the signalling cascade's response to osmotic swelling. The overall results are summarised as $\log(EC_{50})$ values in **Figure 3f**.

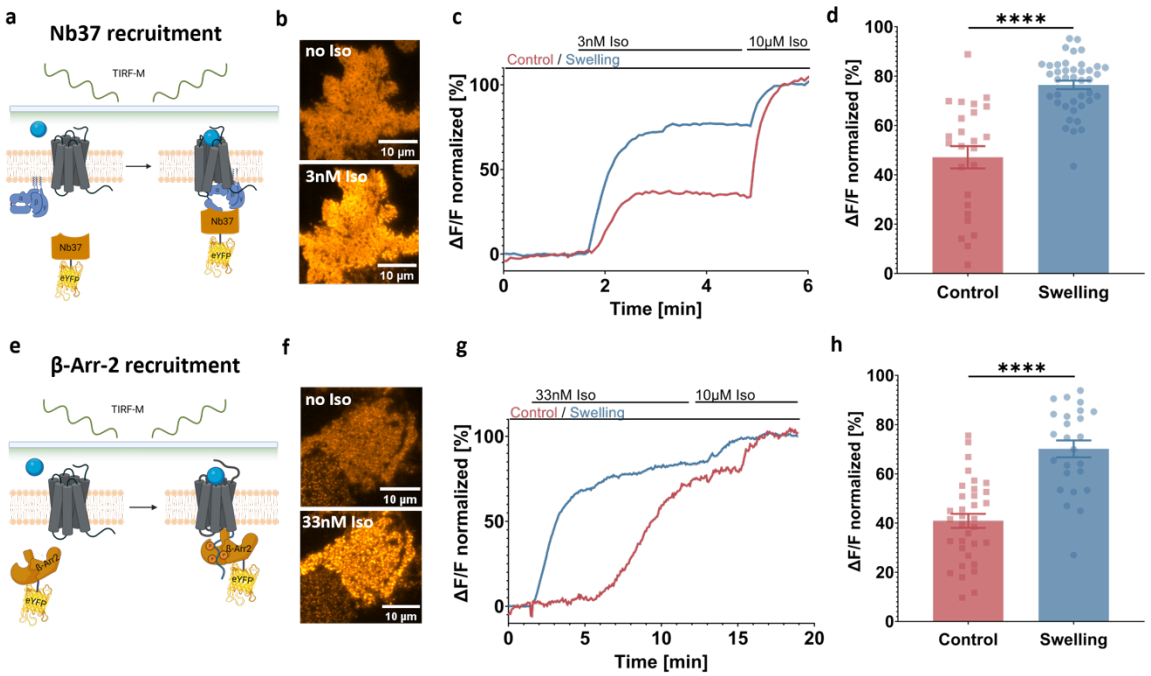

Figure 4 Swelling leads to an increased effector recruitment

a G_s activation by the β2-AR is monitored by recruitment of the fluorescently tagged nanobody 37 (Nb37) at the plasma membrane of the cell together with overexpression of G_s; **b** representative TIRF-M images of Nb37-eYFP expressed in HEK293-AD cells before and after application of 3 nM isoproterenol; **c** representative curve showing relative increase of membrane fluorescence collected as first 3 nM, and then at saturating 10 µM concentration of isoproterenol is added to the cell; **d** relative fluorescence increase measured upon Nb37-eYFP recruitment upon 3 nM isoproterenol stimulation in swollen vs non-swollen cells (mean ± SEM; n = 25 (control) and 41 (swelling) cells from 3 independent experiments; statistical analysis performed by an unpaired two-tailed t-test); **e** recruitment of fluorescently tagged β-Arrestin-2 (β-Arr-2) by the β2-AR is monitored by its recruitment to the plasma membrane of the cell; **f** representative TIRF-M images of βArr-2-eYFP expressed in HEK293-AD cells before and after application of 33 nM isoproterenol; **g** representative curve showing relative increase of membrane fluorescence collected as first 33 nM, and then at saturating 10 µM concentration of isoproterenol is added to the cell; **h** relative fluorescence increase measured upon β-Arr-2-eYFP recruitment upon 33 nM isoproterenol stimulation in swollen vs non-swollen cells (mean ± SEM; n = 34 (control) and 25 (swelling) cells from 3 independent experiments; statistical analysis performed by an unpaired two-tailed t-test).

Based on these observations we decided to investigate further the role of G_s in mediating this remarkable response of cAMP transients to isoproterenol stimulation upon cell swelling. To do so we first asked the question if G_s recruitment to the receptor is enhanced in swollen cells. This question was addressed exploiting fluorescently tagged Nb37[25], reported to bind the active guanine-nucleotide-free $G\alpha_s$, found in the β2-G_s ternary complex, as schematically illustrated in **Figure 4a**. After co-transfecting HEK293AD cells with β2-AR, the heterotrimeric G protein and Nb37-eYFP (as discussed in **Materials and Methods**) we imaged their basolateral membrane using Total Internal Reflection Fluorescence[26], to reject as much as possible, the fluorescence signal from the cytosolic Nb37-eYFP and to enhance the membrane signal. This approach allowed us to monitor the membrane recruitment of Nb37-

eYFP upon increasing concentrations of Iso (**Figure 4b, Supplementary movie 2**), and in turn confirm that in swollen cells the recruitment is enhanced (**Figure 4c**). Overall, the relative recruitment of Nb37 is almost double in swollen cells than in the control (**Figure 4d**). This suggests that in swollen cells there is a sizably higher proportion of active G_s, hinting at a higher number of ternary complexes, and therefore that osmotic swelling is a positive modulator of the receptor active conformation. These measurements are supported by the observation that β-Arrestin-2 recruitment (**Figure 4e,f**), is also enhanced in swollen cells (**Figure 4g**), displaying an almost twofold increase of eYFP-tagged β-Arrestin-2 at the basal cell membrane upon non-saturating isoproterenol stimulation (**Figure 4h**).

If osmotic swelling indeed favors the formation of a ternary ligand-receptor-G_s complex, we expect this to be reflected in a direct modulation of receptor conformation[27]. To test for this possibility, we conducted a set of assays aimed at monitoring ligand binding and receptor activation in intact cells. We employed a recently reported fluorescent ligand against the β-ARs, based on the inverse agonist carazolol[9], to conduct a set of fluorescence anisotropy binding assays[28], as graphically illustrated in **Figure 5a**. As the fluorescence anisotropy increases proportionally to the fraction of bound ligand, it is possible to incubate cells overexpressing β2-AR as well as G_s and Nb37 with a fixed concentration of fluorescent ligand, and then measure changes in fluorescence anisotropy as the fluorescent ligand is progressively displaced by increasing concentrations of the non-fluorescent Iso (**Figure 5b** and **Supplementary Figure 4**). When comparing swollen and control cells, this leads to a small but significant shift in the ligand K_i, from Log(K_i)=-6.77 ± 0.03 to -6.98 ± 0.04 (**Figure 5c**). On the intracellular side the active receptor conformation can be probed by using fluorescently tagged Nb80 (Nb80-eYFP)[29], as schematically described in **Figure 5d**. By employing TIRF to measure nanobody recruitment, we can observe that there is a significant enhancement in Nb80 recruitment in swollen cells (**Figure 5e**), as also reflected by the full concentration response curve's (Log(EC_{50})) shifts from –7.96 ± 0.06 to –8.28 ± 0.09 (**Figure 5g**). Altogether these data confirm that osmotic swelling modulates the β2-AR conformational landscape, favouring an active conformation that in turn leads to an enhanced downstream cAMP cascade.

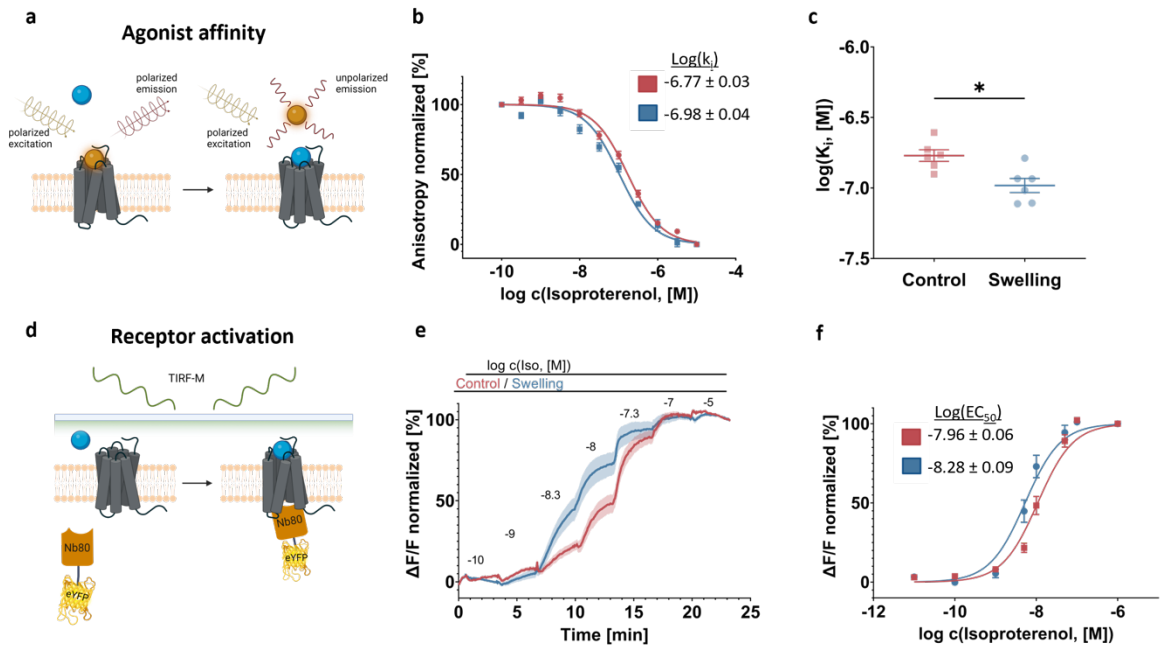

Figure 5 Swelling favors the active receptor conformation

a Ligand binding affinity is determined by employing a fluorescently labelled ligand and measuring the degree of fluorescence anisotropy; **b** average curve of increasing concentrations of isoproterenol displacing 2 nM of fluorescently labelled JE1319 from the β2-AR in swollen and non-swollen cells with the corresponding K_i values **c** scatter plot comparing K_i values obtained from single binding experiments (for **b** and **c** - mean ± SEM; n = 9 plates from 5 independent experiments; statistical analysis by a paired two-tailed t-test) **d** conformational activation of the β2-AR is monitored by recruitment at the plasma membrane of the cell by employing the fluorescently tagged nanobody 80 (Nb80); **e** averaged time-sequence of the relative increase of membrane fluorescence collected as increasing concentration of Isoproterenol are added to the biosensor; **f** the resulting averaged concentration response curves for cells in isotonic and swelling media and associated Log(EC_{50}) values (for **e** and **f** - mean ± SEM; n = 46 (control) and 45 (swelling) cells from 5 independent experiments).

Discussion

Our current understanding of the GPCR signaling cascade, from the ternary complex model down to the more recent structural determination of receptor conformational states, tends to ignore the complexity associated to the cellular environment surrounding a receptor. Cartoons displaying GPCR signalling in textbooks typically highlight the receptor at the membrane, its ligand, and the downstream interaction partner, either the heterotrimeric G protein or, more frequently now, β-arrestins. However, GPCRs are exposed to hundreds of intracellular interactions with other proteins, some already well documented. While the reductionist approach leading to the 'two-state' switch model has been instrumental in our understanding of the function of this important family of receptors, this has in turn allowed us to reach a point where it is now possible to begin investigating the modulatory effects of other, less described, interactions.

In particular, the intracellular domain of plasma membrane GPCRs is exposed to the cell cortex and its distinct organization[30]. In this work we decided to investigate a more general mechanism that can fundamentally alter the cortex and at the same time has a role in several physiological processes, ranging from cardiac ischemia reperfusion[18] to renal function[31], namely osmotic swelling. In our hands, osmotic swelling became a tool to induce pleiotropic changes of the cortex and cell membrane, thereby affecting receptor function. It shall be noted that we explore receptor function in the few minutes upon the onset of osmotic swelling, thus restricting the number of potential effects impacting the signalling cascade to rapid responses, arising from a local reorganization of the membrane and cortex (**Supplementary figure 5**), while excluding more lasting effects such as alterations to gene expression patterns[32].

On this timescale the overall curvature radius of the membrane decreases as the volume increases, while at the same time, small-scale ruffles on the plasma membrane are 'flattened out' together with a remodulation of the actin cortex[33]. Within this scenario, we observe a significant increase in cAMP response in cells undergoing osmotic swelling, and we set to dissect all steps of the β-AR signalling pathway in intact cells, to pinpoint where swelling is having an impact on the signalling cascade.

To do this, we developed, adapted and implemented a wide set of fluorescence spectroscopy techniques that allowed monitoring the activity of each of the signalling partners that support cAMP production and its regulation. Fluorescence cAMP biosensing allowed us to report on the effect (**Figure 1)** in HEK293 cells as well as in the more physiological setting of adult cardiomyocytes (**Figure 2**). This was then combined with specific drug combinations and

knockout cell lines to rule out the role of trafficking (**Figure 3b**), cAMP degradation (**Figure 3c**) or an altered activity of the ACs (**Figure 3d,e**). Indeed, Fsk-induced AC activity appears unchanged in the absence of the G_s, suggesting that a key player in modulating the signalling cascade of the β-ARs is indeed the stimulatory heterotrimeric G protein. To further appreciate how G_s role in transducing receptor signalling is modulated upon osmotic swelling, we employed a fluorescent reporter for the active conformation of $G\alpha_s$, namely eYFP tagged Nb37, a nanobody originally developed to stabilize the structure of the active β2-AR in complex with $G\alpha_s$[34].

With this assay, we can then demonstrate that in swollen cells an equal concentration of agonist leads to an increased number of active receptor-$G\alpha_s$ complexes (**Figure 4a-c**). This result points to improved receptor to G protein coupling as the driving mechanism behind the observed increase in cAMP upon osmotic swelling. According to the ternary complex model[1], we thus investigated the possibility that osmotic swelling stabilizes the active receptor conformation first by monitoring ligand binding in intact cells (**Figure 5a**) and then by a proxy for G protein coupling, namely the Nb80, originally reported to stabilize the active receptor conformation[29] (**Figure 5d**).

Upon ligand displacement experiments, the measured k_d displays a statistically significant change in swollen cells (**Figure 5b-c**), with increased affinity of the receptors towards isoproterenol in swollen cells. Moreover, the enhancement in Nb80 recruitment upon swelling displayed in **Figure 5e-f** corroborates the notion that receptors active conformation is indeed favoured by osmotic swelling.

Overall, these results point to a modulation of receptor activity upon cell swelling, that we ascribe to cell swelling favouring the active conformation of the β2-AR. This observation would agree with a recent report suggesting that osmotic swelling leads to increased hydration of the intracellular side of the receptor, 'forcing open' the G protein binding pocket and thus favouring coupling[35]. Other explanations, such as an enhanced 'collision coupling' of the receptor to the G protein[36], are possible: while we observed a slight increase in receptor diffusion coefficients, we did not measure any increase in G protein ($G\alpha_s$) diffusion rate in swollen cells as opposed to control (data not shown). Since osmotic swelling has broad effects on the cell cortex and plasma membrane, such as actin remodelling, altered lipid composition, as well as changes in both local (flattening of ruffles and invaginations) and low (overall increase in volume) geometrical curvature[32], we believe it is difficult to pinpoint its effect as one specific molecular mechanism. Nonetheless, our observation with other G_s-coupled receptors as well as with the G_i coupled μOR, point to the generality of this regulatory mechanism. These results suggest that osmotic cell volume changes can be intrinsic modulators of GPCR activity in several contexts of pathophysiological relevance, ranging from cardiac ischemia-reperfusion to the reported swelling of adipocytes[37]. Further studies and more refined biophysical approaches will be needed to deconvolve the specific molecular mechanisms mediating the effects of a perturbation such as osmotic swelling at the level of the isolated receptor.

Materials and Methods

Cell culture. HEK293 and HEK293 derived cells (Epac-S^{H187} stable cell line, HEK293AD, $G\alpha_s$-KO cell line) were cultured in DMEM medium containing 4.5 g/l glucose (Gibco) supplemented with 10% fetal calf serum (FSC, Biochrome), 2 mM l-glutamine, 100 units/ml penicillin and 0.1 mg/ml streptomycin, at 37 °C, 5% CO_2. To split cells, growth medium was removed by aspiration and cells were washed once with 10 ml of PBS (Sigma), followed by trypsinization

for 2 min in 1.5 ml of trypsin 0.05%/EDTA 0.02% (PAN Biotech) solution and resuspended in the desired amount of DMEM medium.

Transfection. For the single cell microscopy experiments the cells were transfected directly in the imaging dishes 24 hours prior to conducting the experiments, using JetPrime transfection reagent (Polyplus) according to manufacturer's protocol. For the plate reader experiments the cells were transfected on 10 cm plates 48 hours before the experiment using a reduced amount of JetPrime transfection reagent and total DNA (5µl and 2.5µg respectively) and transferred to black 96-well plates (Brandt) 24 hours before the experiment. The transfected cDNA and cDNA ratios for co-transfections are listed in further sections.

Molecular cloning. The tricistronic G_s and G_s-CFP plasmids were created using NEBuilder HiFi DNA assembly cloning kit (NEB). $G\alpha_s$ (or $G\alpha_s$-CFP[38]), $G\beta_1$ and $G\gamma_2$ were cloned into the pcDNA3(+) backbone following the same structure as for the published G_i FRET sensors [16]: $G\beta_1$-2A-$G\gamma_2$-IRES-$G\alpha_s$ (or $G\alpha_s$-CFP respectively).

Swelling medium. Throughout all experiments two types of imaging buffers (control – mannitol electrolyte solution 300 mOsm (MES300) and swelling – mannitol electrolyte solution 200 mOsm (MES200)) were used. A basic buffer with a low osmolarity – ES150 – was produced by solving 60 mM NaCl, 5 mM KCl, 2 mM $CaCl_2$, 1 mM $MgCl_2$, 10 mM HEPES in distilled water and resulting in electrolyte solution 150 mOsm (ES150). It was than supplemented with 150 mM mannitol (Sigma) to produce MES300 and reach 300 mOsm. MES300 was then used for washing and incubation steps as described in specific experiments. To achieve hypotonic conditions of 200 mOsm during the experiments, 2/3 of the total volume of MES300 was removed from the wells and replaced with the same volume of ES150, resulting in MES200. In control condition 2/3 of MES300 were also removed and replaced with fresh MES300 to avoid ascribing any effects to mechanical artifacts.

Cardiomyocyte isolation. Cardiomyocyte isolation involved obtaining cardiac myocytes from adult ventricles of CAG-Epac1-camps mice aged 8 to 12 weeks[9], regardless of their gender. The process employed enzymatic collagen digestion and retrograde perfusion through the aorta using a Langendorff perfusion apparatus, as previously described[9]. In brief, the hearts were swiftly removed from the mice after cervical dislocation and connected to a custom-built perfusion system. Initially, the hearts were perfused with perfusion buffer for 4 minutes at a rate of 3 ml/min, followed by an 8-minute perfusion with myocyte digestion buffer containing 5 mg of liberase dispase high DH enzyme (Roche) per digestion. Subsequently, the heart was detached from the perfusion system, and the ventricles were dissected into small pieces using scalpels. After sedimentation, removal of the supernatant, and resuspension the cells were filtered through a nylon mesh cell strainer (100-µm pore size, Falcon) to eliminate any remaining tissue fragments. The cells were then gradually exposed to physiological Ca^{2+} concentrations (~1 mM), resuspended in myocyte plating medium, and seeded on freshly coated Matrigel-coated 8-well Ibidi µ-slides for each experiment. More detailed information about the buffers and materials used can be found in the methods section of Bathe-Peters et al[9].

Cell area measurements with confocal microscopy. To measure the effect of hypotonic treatment on cell area murine cardiomyocytes were seeded in 8-well Ibidi µ-slides with a density of 1,000 cells per well and labeled with Cell Mask™ Deep Red according to manufacturer's protocol. XY and XZ movies of cells were then aquired on a confocal laser scanning microscope, Leica SP8, with a white-light laser at the wavelength of 633 nm and laser power of 5%. All measurements were conducted with an HC PLAP CS2 40×1.3 numerical aperture (NA) oil immersion objective (Leica). Movies were aquired at 30 seconds per frame with a hybrid detector in the range of 643 to 693 nm. Medium change to induce

swelling was performed as described in previous sections. ImageJ was used to conduct thresholding and object detection on the cells and the extracted area was plotted with Prism v. 9.5.1.

FRET microscopy. HEK293 cells stably expressing Epac-S^{H187} sensor were seeded in 8-well Ibidi µ-slides with a density of 25,000 cells per well. Cells were washed twice in MES300 and imaged at room temperature. An inverted microscope (DMi8, Leica Microsystems), equipped with an x63 HC PL APO, 1.40-0.60 numerical aperture (NA) objective (Leica Microsystems), dichroic beamsplitter T505lpxr (Visitron Systems), xenon lamp coupled with a continuously tunable Visichrome high-speed polychromator (Visitron Systems) and a metal-oxide-semiconductor camera (Prime95B, Teledyne Photometrics) with a dual image splitter (OptoSplit II, Cairn Research), was used. Excitation wavelength of 445 nm was used and fluorescence emission was simultaneously recorded at 470/24 nm and 535/30 nm. The movies were obtained at 5 seconds per frame for the number of frames needed for the cAMP concentrations to equilibrate. ImageJ was used to extract fluorescence intensity values from single cells, which were corrected for background and used to calculate FRET/CFP ratio.

Plate reader cAMP FRET measurements. HEK293 cells stably expressing Epac-S^{H187} sensor were seeded in black 96-well plates (Brand) with a density of 50,000 cells per well. 24 h later cells were washed twice with 90 µl MES300 per well. After 5 min incubation at 37°C, baseline measurement was conducted in a Neo2 plate reader (Biotek) using 420 nm excitation and 485 nm / 540 nm emission filters. As the second step, 60 µl MES300 were removed from each well and replaced with 60 µl of either MES300 or ES150 for the “control” and “swelling” conditions respectively and the plate was measured for 15 minutes. Afterwards the desired dilution series with increasing concentrations of ligand was added (10 µl per well of a 10x concentration in MES300) and the plate was measured again for 15 minutes. At last, a mix of forskolin/IBMX in MES300 was added to an end concentration of 10 µM forskolin and 100 µM IBMX and measured for 10 more minutes. The change in acceptor/donor ratio was normalized to 0% baseline and 100% forskolin/IBMX and plotted in Prism v.9.5.1. For the concentration response curves “Dose-response stimulation fit (three parameters)” was applied.

TIRF microscopy. HEK293AD cells were seeded in 8-well Ibidi® µ-slides with a density of 25,000 cells per well and transfected with JetPrime® transfection according to manufacturer’s protocol. Following cDNA ratios were used: for Nb80 recruitment – 9x Snap-ß2AR and 1x Nb80-eYFP; for Nb37 recruitment – 1x Snap-ß2AR, 1x $G\beta_1$-2A-$G\gamma_2$-IRES-$G\alpha_s$ and 3x Nb37-eYFP; Transfected cells were labeled with 1 µM SNAP-Surface 674 dye (NEB) for 30 min followed by washing two times for 10 min with 300 µl MES300 per well. After labeling, cells were subsequently taken for imaging to an Attofluor cell chamber (Fisher Scientific) in MES300. A TIRF illuminated Eclipse Ti2 microscope (Nikon), equipped with a x100, 1.49 NA automated correction collar objective and 405-, 488-, 561-, 647-nm laser diodes coupled via an automated N-Storm module and four iXon Ultra 897 EMCCD cameras (Andor), was used. Objective and cell chamber were kept at 37°C during imaging. The automated objective collar was on and hardware autofocus was activated. Movies were acquired at 4 s per frame for 400 frames. After a baseline measurement of 50 frames increasing concentrations of isoproterenol were added to the imaged well in 50 frame steps. Prior to each isoproterenol addition 30 µl of solution was removed from the well and 30 µl of 10x isoproterenol in either MES300 or MES200 was applied. ImageJ was used to extract fluorescence intensity values, which were corrected for background and normalized to 0% baseline and 100% 10 µm isoproterenol stimulation. In case of F-actin content measurment HEK293AD cells were transfected with Lifeact-eGFP and imaged as described above at 30 seconds per frame.

Plate reader ligand binding assays. HEK293T cells were seeded in 10 cm culture plates, co-transfected with 1x Snap-ß2AR, 1x Nb37-eYFP and 3x $G\beta_1$-2A-$G\gamma_2$-IRES-$G\alpha_s$-CFPafter 24

h and reseeded in black 96-well plates with a density of 50,000 cells per well another 24 h later. The plate was incubated with 100 ul MES300 containing 2 nM JE1319. As the second step, 60 µl MES300 was removed from each well and replaced with 60 µl of either MES300 or ES150 (both containing 2 nM JE1319) for the "control" and "swelling" conditions respectively and the plate was incubated for further 15 minutes. Afterwards the desired dilution series with increasing concentrations of isoproterenol was added (10 µl per well of a 10x concentration in MES300) and the plate was incubated for 90 minutes and measured in a Neo2 plate reader (Biotek) using DualFP polarization filter and an 620 nm/680 nm excitation/emission filter. A G-factor of 0.12 was measured for the instrument. Fluorescence anisotropy was calculated as $r = (I_{\parallel} - I_{\perp})/(I_{\parallel} + 2I_{\perp})$ and plotted in Prism v.9.5.1. For the concentration response curves "Dose-response inhibition fit was applied with min and max being constrained to 0% and 100% respectively.

Plate reader G_i-FRET sensor assay. HEK293T cells were seeded in 10 cm cell culture dishes at a density of 4×10^6. Cells were co-transfected with 1x SNAP-µOR and 4x G_{i2} FRET sensor 24 h after seeding, as described in previous sections; 24 h after transfection, cells were trypsinized and transferred into black 96-well plates (Brand), at a density of 50,000 cells per well; 16 h to 24 h later, cells were washed with MES300, and then 90 µl of MES300 was added to each well. After 10 min incubation at 37 °C, measurement was performed at 37 °C using a Synergy Neo2 Plate Reader (Biotek) using a CFP/YFP FRET filter set. After basal FRET measurement, medium was changed as described above and after 15 minutes of further measurement 10 µl of ligand solution were applied to each well. The change in acceptor/donor ratio was normalized to 0% baseline and plotted in Prism v.9.5.1. For the concentration response curves "Dose-response stimulation fit (three parameters)" was applied.

Acknowledgments

This project was supported by the Deutsche Forschungsgemeinschaft (DFG), via collaborative research center 1423 Project 421152132, Subproject C03 (to P.A. and M.J.L.).

We are grateful to Bärbel Pohl, Marlies Grieben and Ulrike Zabel for their excellent technical assistance. We would like to acknowledge Heike Biebermann (Charité UniversitätsMedizin, Berlin) for kindly sharing the HEK293 cells stably expressing Epac1-S^{H187}, and Peter Gmeiner (Friedrich-Alexander-Universität, Erlangen) for sharing the ligand JE1319. Nb80 and Nb37 plasmids were a gift from Mark von Zastrow. Epac1-S^{H187} biosensor plasmid was a gift from Kees Jalink (The Netherlands Cancer Institute, Amsterdam). We are grateful to Romy Thomas (Max Delbrück Center, Berlin) for helping us generate the tricistronic heterotrimeric G protein expression vector used in our experiments.

Author contributions

A.S. and P.A. designed research; A.S. performed research; A.I. contributed new reagents/analytic tools; A.S. and P.A. analyzed data; M.B.-P. supported the preparation of primary cardiomyocytes; P.A and M.J.L. supervised the project and acquired funding; P.A. and A.S. wrote the paper with input from all authors.

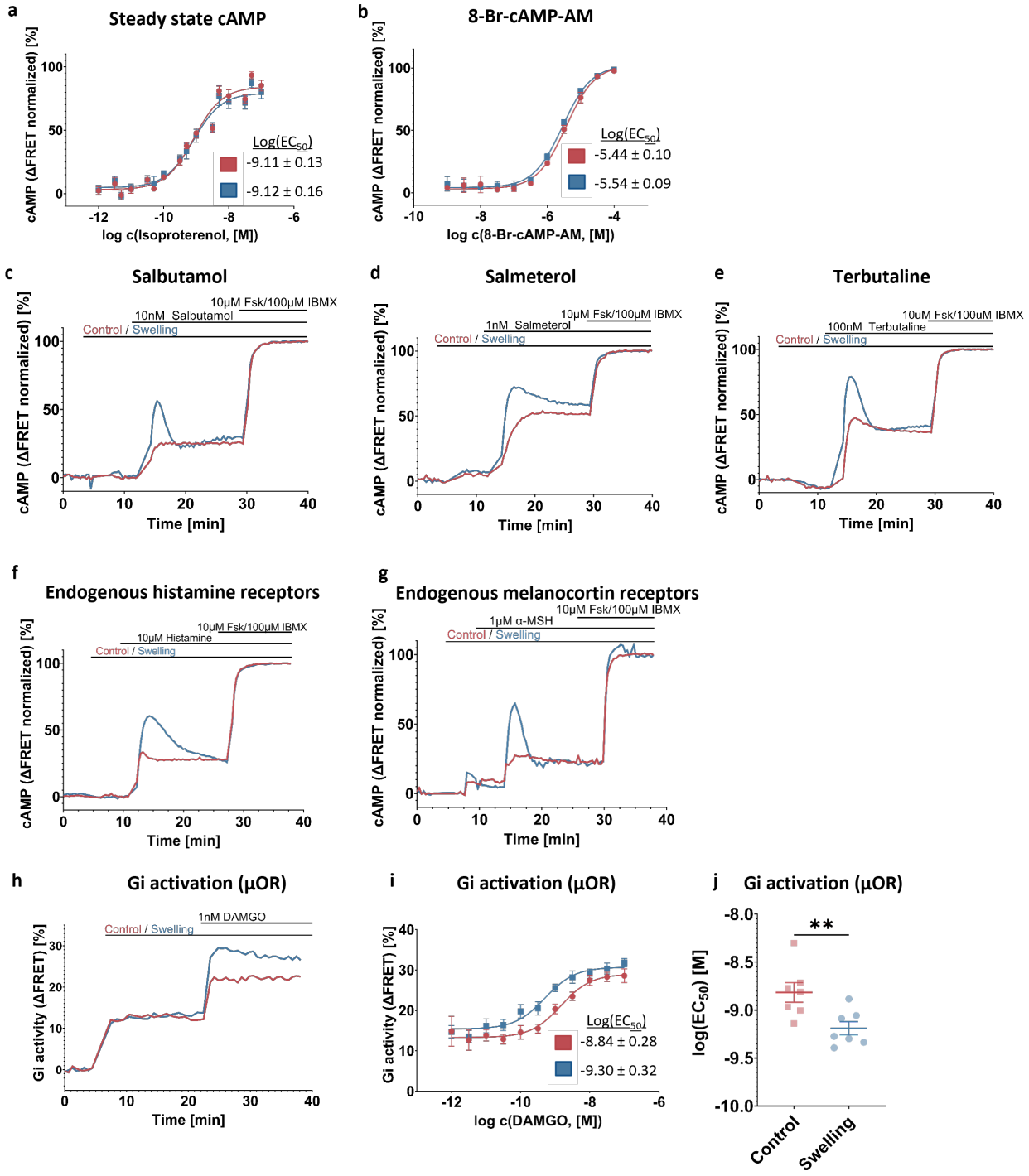

Supp. Fig. 1: Effect of swelling on receptor signaling is generalizable to other ß-AR agonists, to other G_s-coupled GPCRs and to the G_i pathway a averaged concentration response curves representing steady state cAMP concentrations, as indicated in (**Fig1. c**) (mean ± SEM; n = 6 independent experiments); **b** averaged concentration response curves of Epac-S^{H187} stable cell line being stimulated by increasing concentrations of 8-Br-cAMP-AM (mean ± SEM; n = 3 independent experiments); **c-e** representative curves showing kinetic cAMP concentrations as a response to different ß-adrenergic agonists in Epac-S^{H187} stable cells (normalized to baseline and 10μM Forskolin + 100μM IBMX); **f,g** representative curves showing kinetics cAMP concentrations as a response to histamine (**f**) and α-MSH (**g**) in Epac-S^{H187} stable cells (normalized to baseline and 10μM Forskolin + 100μM IBMX); **h-j** representative curve (**h**), averaged concentration response curve (**i**) and $logEC_{50}$ values from

individual experiments (**j**) comparing a Gi2 FRET-sensor response to DAMGO in control and swollen cells, transiently transfected with μOR and G_{i2}-FRET sensor.

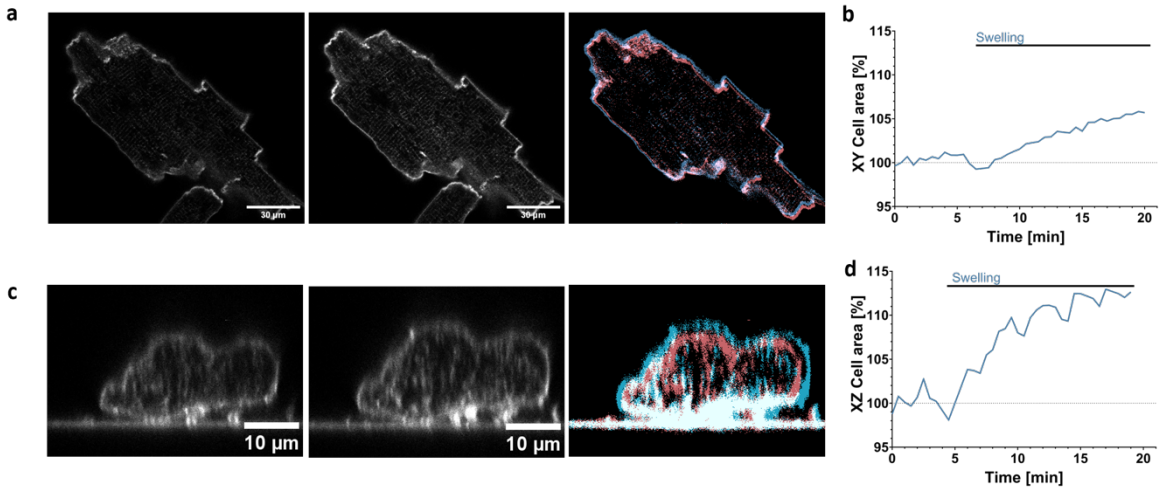

Supp. Fig. 2: Characterization of cardiomyocyte swelling

a-d Confocal images of CM under isotonic conditions (left) and after 20 minutes of exposure to swelling medium (middle), with an overlay of cell edges under both conditions (right) and the quantification of cell area imaged in XY plane (**a,b**) and XZ plane (**c,d**);

Supplementary movie 1 (cAMP in CM upon Iso and Fsk/IBMX stimulation)

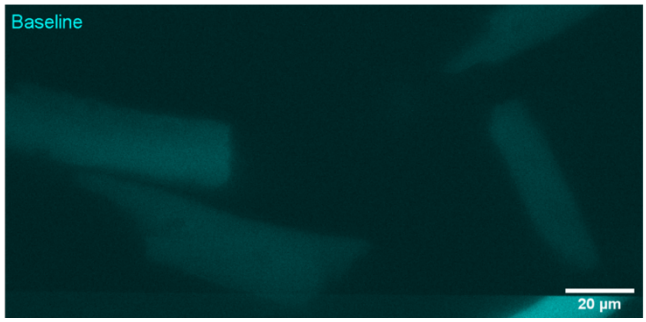

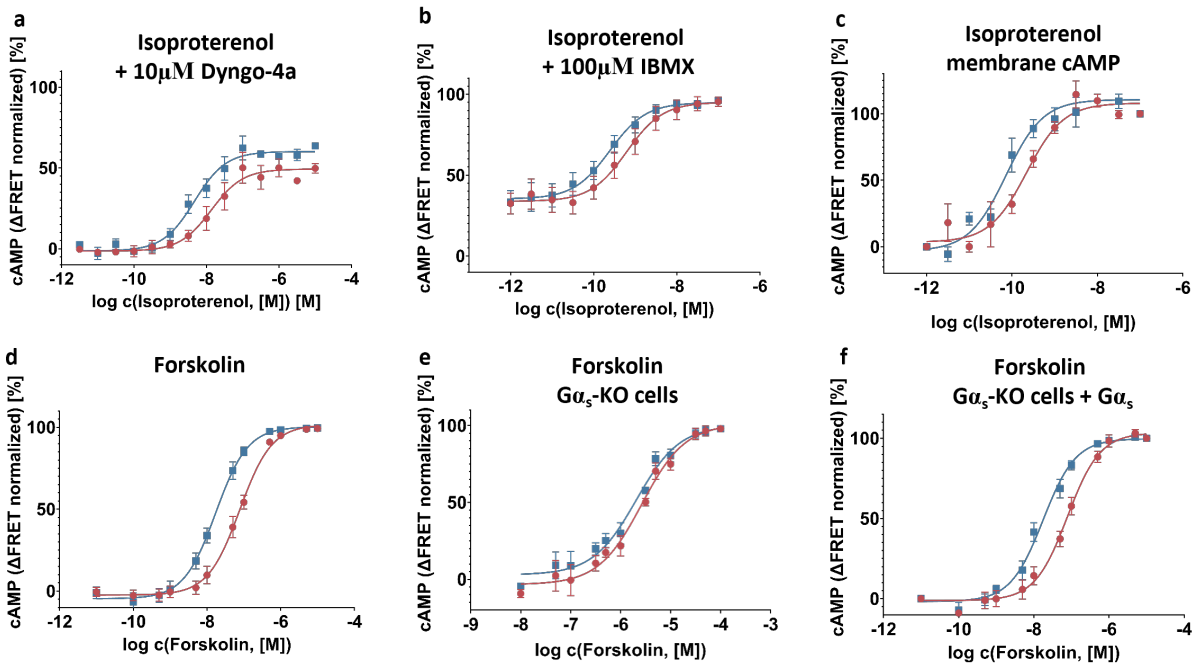

Supp. Fig. 3: Impact of cell swelling on isoprenaline potency under selective regulation of the β-adrenergic signalling cascade

a-f averaged concentration response curves of intracellular cAMP concentrations under following conditions: (**a**) cytosolic cAMP measured upon Iso stimulation after treatment with 10 µM Dyngo4a for 30 min; (**b**) cytosolic cAMP measured upon Iso stimulation with simultaneous addition of 100µM IBMX; (**c**) local cAMP at the plasma membrane upon Iso stimulation measured with an Epac-Camps1-Caax sensor; (**d,e,f**) cytosolic cAMP measured upon Fsk stimulation in wt $G\alpha_s$ phenotype (**d**), $G\alpha_s$-KO cells (**e**) and $G\alpha_s$-KO cells transiently transfected with $G\alpha_s$ (**f**)

Supplementary movie 2 (Nb37-eYFP recruitment)

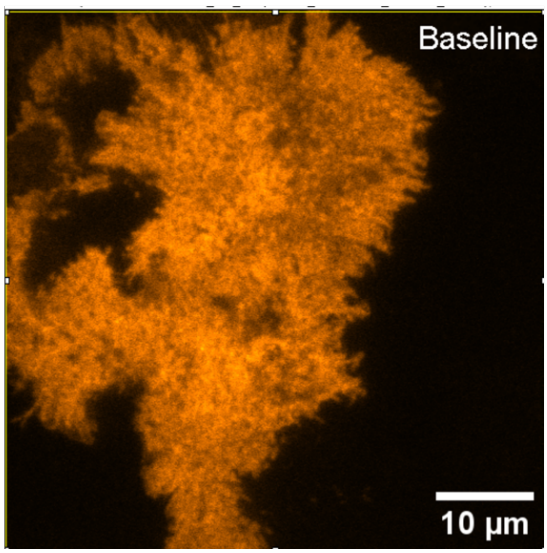

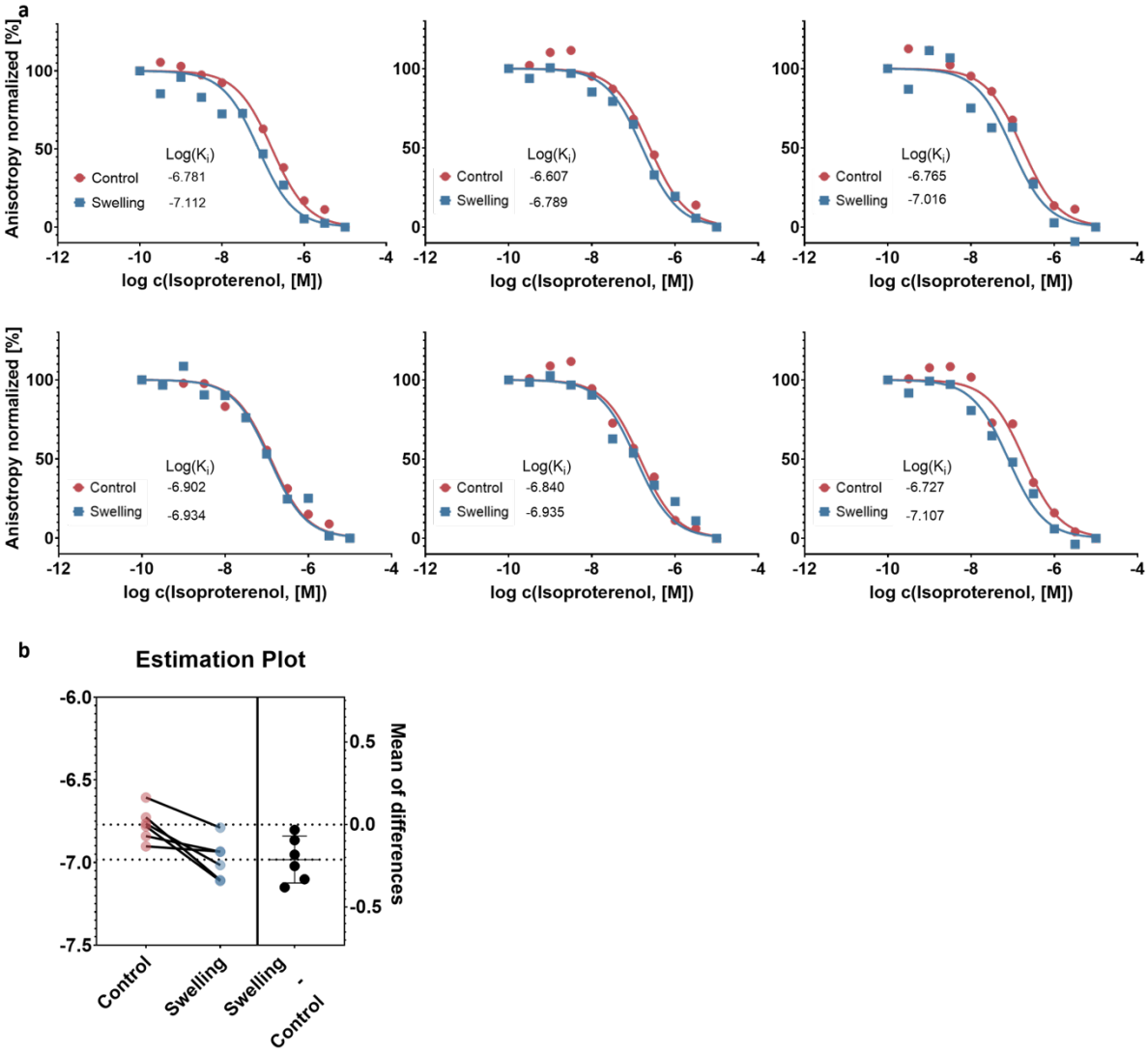

Supp. Fig. 4: Fluorescence anisotropy measurements show an increase of isoproterenol binding affinity in swollen cells

a single displacement curves from individual experiments, averaged in **Fig. 5 (b) b** pairwise comparison of log (Kd) values represented in **Fig. 5c,** comparing swollen to control cells, and the average of the difference overlay.

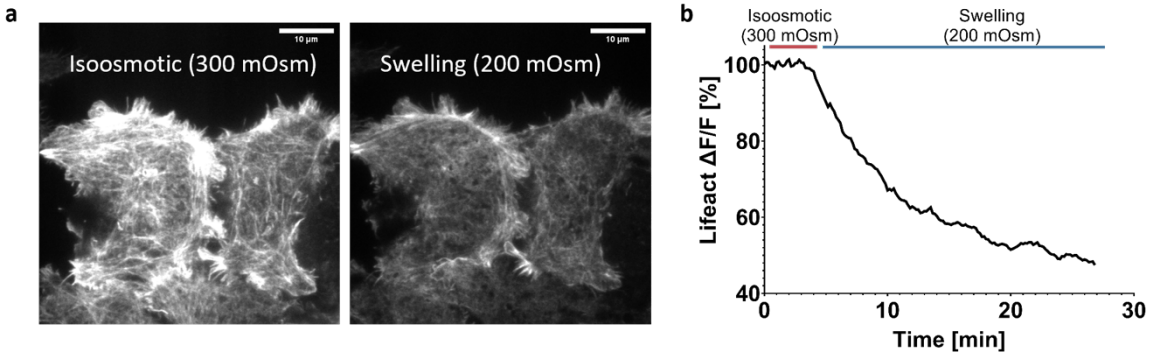

Supp. Fig. 5: F-actin labeling shows a decrease in cortical actin polymerization upon induction of cell swelling

a representative TIRF-M images of HEK293 cells transfected with Lifeact-eGFP and visualizing F-actin in basal conditions (left) and after 20 minutes of incubation in swelling medium (right) **b** quantification of Lifeact-eGFP intensity over the course of time for one representative cell

References

1 De Lean, A., Stadel, J. M. & Lefkowitz, R. J. A ternary complex model explains the agonist-specific binding properties of the adenylate cyclase-coupled beta-adrenergic receptor. *J Biol Chem* **255**, 7108-7117 (1980).

2 Shukla, A. K., Singh, G. & Ghosh, E. Emerging structural insights into biased GPCR signaling. *Trends Biochem Sci* **39**, 594-602 (2014). https://doi.org:10.1016/j.tibs.2014.10.001

3 Leach, K., Sexton, P. M. & Christopoulos, A. Allosteric GPCR modulators: taking advantage of permissive receptor pharmacology. *Trends Pharmacol Sci* **28**, 382-389 (2007). https://doi.org:10.1016/j.tips.2007.06.004

4 Hay, D. L., Poyner, D. R. & Sexton, P. M. GPCR modulation by RAMPs. *Pharmacol Ther* **109**, 173-197 (2006). https://doi.org:10.1016/j.pharmthera.2005.06.015

5 Oates, J. & Watts, A. Uncovering the intimate relationship between lipids, cholesterol and GPCR activation. *Curr Opin Struct Biol* **21**, 802-807 (2011). https://doi.org:10.1016/j.sbi.2011.09.007

6 Cao, T. T., Deacon, H. W., Reczek, D., Bretscher, A. & von Zastrow, M. A kinase-regulated PDZ-domain interaction controls endocytic sorting of the beta2-adrenergic receptor. *Nature* **401**, 286-290 (1999). https://doi.org:10.1038/45816

7 Soubias, O., Teague, W. E., Hines, K. G. & Gawrisch, K. The role of membrane curvature elastic stress for function of rhodopsin-like G protein-coupled receptors. *Biochimie* **107 Pt A**, 28-32 (2014). https://doi.org:10.1016/j.biochi.2014.10.011

8 Rosholm, K. R. *et al.* Membrane curvature regulates ligand-specific membrane sorting of GPCRs in living cells. *Nat Chem Biol* **13**, 724-729 (2017). https://doi.org:10.1038/nchembio.2372

9 Bathe-Peters, M. *et al.* Visualization of beta-adrenergic receptor dynamics and differential localization in cardiomyocytes. *Proc Natl Acad Sci U S A* **118** (2021). https://doi.org:10.1073/pnas.2101119118

10 Calebiro, D. *et al.* Persistent cAMP-signals triggered by internalized G-protein-coupled receptors. *PLoS Biol* **7**, e1000172 (2009). https://doi.org:10.1371/journal.pbio.1000172

11 Ostrom, R. S. & Insel, P. A. The evolving role of lipid rafts and caveolae in G protein-coupled receptor signaling: implications for molecular pharmacology. *Br J Pharmacol* **143**, 235-245 (2004). https://doi.org:10.1038/sj.bjp.0705930

12 Romero, G., von Zastrow, M. & Friedman, P. A. Role of PDZ proteins in regulating trafficking, signaling, and function of GPCRs: means, motif, and opportunity. *Adv Pharmacol* **62**, 279-314 (2011). https://doi.org:10.1016/B978-0-12-385952-5.00003-8

13 Scarselli, M. *et al.* Revealing G-protein-coupled receptor oligomerization at the single-molecule level through a nanoscopic lens: methods, dynamics and biological function. *FEBS J* **283**, 1197-1217 (2016). https://doi.org:10.1111/febs.13577

14 Liu, X. *et al.* Structural Insights into the Process of GPCR-G Protein Complex Formation. *Cell* **177**, 1243-1251 e1212 (2019). https://doi.org:10.1016/j.cell.2019.04.021

15 Scarselli, M., Annibale, P. & Radenovic, A. Cell type-specific beta2-adrenergic receptor clusters identified using photoactivated localization microscopy are not lipid raft related, but depend on actin cytoskeleton integrity. *J Biol Chem* **287**, 16768-16780 (2012). https://doi.org:10.1074/jbc.M111.329912

16 van Unen, J. *et al.* A New Generation of FRET Sensors for Robust Measurement of Galphai1, Galphai2 and Galphai3 Activation Kinetics in Single Cells. *PLoS One* **11**, e0146789 (2016). https://doi.org:10.1371/journal.pone.0146789

17 Klarenbeek, J., Goedhart, J., van Batenburg, A., Groenewald, D. & Jalink, K. Fourth-generation epac-based FRET sensors for cAMP feature exceptional brightness, photostability and dynamic range: characterization of dedicated sensors for FLIM, for ratiometry and with high affinity. *PLoS One* **10**, e0122513 (2015). https://doi.org:10.1371/journal.pone.0122513

18 Vandenberg, J. I., Rees, S. A., Wright, A. R. & Powell, T. Cell swelling and ion transport pathways in cardiac myocytes. *Cardiovasc Res* **32**, 85-97 (1996).
19 Nikolaev, V. O., Bunemann, M., Hein, L., Hannawacker, A. & Lohse, M. J. Novel single chain cAMP sensors for receptor-induced signal propagation. *J Biol Chem* **279**, 37215-37218 (2004). https://doi.org:10.1074/jbc.C400302200
20 Nikolaev, V. O., Bunemann, M., Schmitteckert, E., Lohse, M. J. & Engelhardt, S. Cyclic AMP imaging in adult cardiac myocytes reveals far-reaching beta1-adrenergic but locally confined beta2-adrenergic receptor-mediated signaling. *Circ Res* **99**, 1084-1091 (2006). https://doi.org:10.1161/01.RES.0000250046.69918.d5
21 Drake, M. T., Shenoy, S. K. & Lefkowitz, R. J. Trafficking of G protein-coupled receptors. *Circ Res* **99**, 570-582 (2006). https://doi.org:10.1161/01.RES.0000242563.47507.ce
22 Beavo, J. A. *et al.* Effects of xanthine derivatives on lipolysis and on adenosine 3',5'-monophosphate phosphodiesterase activity. *Mol Pharmacol* **6**, 597-603 (1970).
23 Anton, S. E. *et al.* Receptor-associated independent cAMP nanodomains mediate spatiotemporal specificity of GPCR signaling. *Cell* **185**, 1130-1142 e1111 (2022). https://doi.org:10.1016/j.cell.2022.02.011
24 Stallaert, W. *et al.* Purinergic Receptor Transactivation by the beta(2)-Adrenergic Receptor Increases Intracellular Ca(2+) in Nonexcitable Cells. *Mol Pharmacol* **91**, 533-544 (2017). https://doi.org:10.1124/mol.116.106419
25 Westfield, G. H. *et al.* Structural flexibility of the G alpha s alpha-helical domain in the beta2-adrenoceptor Gs complex. *Proc Natl Acad Sci U S A* **108**, 16086-16091 (2011). https://doi.org:10.1073/pnas.1113645108
26 Axelrod, D. Total internal reflection fluorescence microscopy. *Methods Cell Biol* **30**, 245-270 (1989). https://doi.org:10.1016/s0091-679x(08)60982-6
27 Nygaard, R. *et al.* The dynamic process of beta(2)-adrenergic receptor activation. *Cell* **152**, 532-542 (2013). https://doi.org:10.1016/j.cell.2013.01.008
28 Lakowicz, J. R. *Principles of fluorescence spectroscopy*. 2nd edn, (Kluwer Academic/Plenum, 1999).
29 Rasmussen, S. G. *et al.* Structure of a nanobody-stabilized active state of the beta(2) adrenoceptor. *Nature* **469**, 175-180 (2011). https://doi.org:10.1038/nature09648
30 Koster, D. V. & Mayor, S. Cortical actin and the plasma membrane: inextricably intertwined. *Curr Opin Cell Biol* **38**, 81-89 (2016). https://doi.org:10.1016/j.ceb.2016.02.021
31 Haussinger, D. The role of cellular hydration in the regulation of cell function. *Biochem J* **313 (Pt 3)**, 697-710 (1996). https://doi.org:10.1042/bj3130697
32 Lang, F. *et al.* Functional significance of cell volume regulatory mechanisms. *Physiol Rev* **78**, 247-306 (1998). https://doi.org:10.1152/physrev.1998.78.1.247
33 Groulx, N., Boudreault, F., Orlov, S. N. & Grygorczyk, R. Membrane reserves and hypotonic cell swelling. *J Membr Biol* **214**, 43-56 (2006). https://doi.org:10.1007/s00232-006-0080-8
34 Irannejad, R. *et al.* Conformational biosensors reveal GPCR signalling from endosomes. *Nature* **495**, 534-538 (2013). https://doi.org:10.1038/nature12000
35 Fried, S. D. E. *et al.* Hydration-mediated G-protein-coupled receptor activation. *Proc Natl Acad Sci U S A* **119**, e2117349119 (2022). https://doi.org:10.1073/pnas.2117349119
36 Tolkovsky, A. M. & Levitzki, A. Mode of coupling between the beta-adrenergic receptor and adenylate cyclase in turkey erythrocytes. *Biochemistry* **17**, 3795 (1978). https://doi.org:10.1021/bi00611a020
37 Hoffmann, E. K., Lambert, I. H. & Pedersen, S. F. Physiology of cell volume regulation in vertebrates. *Physiol Rev* **89**, 193-277 (2009). https://doi.org:10.1152/physrev.00037.2007
38 Hynes, T. R., Mervine, S. M., Yost, E. A., Sabo, J. L. & Berlot, C. H. Live cell imaging of Gs and the beta2-adrenergic receptor demonstrates that both alphas and beta1gamma7 internalize upon stimulation and exhibit similar trafficking patterns that differ from that of the beta2-

adrenergic receptor. *J Biol Chem* **279**, 44101-44112 (2004).
https://doi.org:10.1074/jbc.M405151200